Hybrid Application of Nanoparticles and Polymer in Enhanced Oil Recovery Processes

Hu, Yanqiu; Zhao, Zeyuan; Dong, Huijie; Mikhailova, Maria Vladimirovna; Davarpanah, Afshin

Published in:
Polymers

DOI:
10.3390/polym13091414

Publication date:
2021

Citation for published version (APA):
Hu, Y., Zhao, Z., Dong, H., Mikhailova, M. V., & Davarpanah, A. (2021). Hybrid Application of Nanoparticles and Polymer in Enhanced Oil Recovery Processes. *Polymers*, *13*(9), [1414]. https://doi.org/10.3390/polym13091414

polymers

MDPI

Article

Hybrid Application of Nanoparticles and Polymer in Enhanced Oil Recovery Processes

Yanqiu Hu [1,*], Zeyuan Zhao [1], Huijie Dong [1], Maria Vladimirovna Mikhailova [2] and Afshin Davarpanah [3,*]

[1] The Pharmaceutical College of Jiamusi University, Jiamusi University, Jiamusi 154007, China; zhaozeyuan@jmsu.edu.cn (Z.Z.); donghuijie@jmsu.edu.cn (H.D.)
[2] Department of Prosthetic Dentistry, Sechenov First Moscow State Medical University, 119992 Moscow, Russia; sfmsmu@mail.ru
[3] Department of Mathematics, Aberystwyth University, Aberystwyth SY23 3BZ, UK
* Correspondence: huyanqiu@jmsu.edu.cn (Y.H.); afd6@aber.ac.uk (A.D.)

Abstract: Nowadays, the addition of nanoparticles to polymer solutions would be of interest; however, the feasible property of nanoparticles and their impact on oil recovery has not been investigated in more detail. This study investigates the rheology and capillary forces (interfacial tension and contact angle) of nanoparticles in the polymer performances during oil recovery processes. Thereby, a sequential injection of water, polymer, and nanoparticles; Nanosilica (SiO_2) and nano-aluminium oxide (Al_2O_3) was performed to measure the oil recovery factor. Retention decrease, capillary forces reduction, and polymer viscoelastic behavior increase have caused improved oil recovery due to the feasible mobility ratio of polymer–nanoparticle in fluid loss. The oil recovery factor for polymer flooding, polymer–Al_2O_3, and polymer–SiO_2 is 58%, 63%, and 67%, respectively. Thereby, polymer–SiO_2 flooding would provide better oil recovery than other scenarios that reduce the capillary force due to the structural disjoining pressure. According to the relative permeability curves, residual oil saturation (S_{or}) and water relative permeability (K_{rw}) are 29% and 0.3%, respectively, for polymer solution; however, for the polymer–nanoparticle solution, S_{or} and K_{rw} are 12% and 0.005%, respectively. Polymer treatment caused a dramatic decrease, rather than the water treatment effect on the contact angle. The minimum contact angle for water and polymer treatment are about 21 and 29, respectively. The contact angle decrease for polymer treatment in the presence of nanoparticles related to the surface hydrophilicity increase. Therefore, after 2000 mg L^{-1} of SiO_2 concentration, there are no significant changes in contact angle.

Keywords: polymer solution; nanoparticles; interfacial tension; oil recovery factor; relative permeability curves

Citation: Hu, Y.; Zhao, Z.; Dong, H.; Vladimirovna Mikhailova, M.; Davarpanah, A. Hybrid Application of Nanoparticles and Polymer in Enhanced Oil Recovery Processes. *Polymers* **2021**, *13*, 1414. https://doi.org/10.3390/polym13091414

Academic Editors: Motoyoshi Kobayashi and Piotr Warszyński

Received: 12 March 2021
Accepted: 23 April 2021
Published: 27 April 2021

1. Introduction

Petroleum industries tried to increase the oil production from underground hydrocarbon fields due to the global energy demand in various industries and crude oil and its components [1–16]. Thereby, to provide a sustainable demand, new technologies and advancements should be applied to increase oil production [17–25]. Moreover, it has always been challenging for petroleum industries, as natural drive mechanisms would not be efficient [26–32]. Enhanced oil recovery and improved oil recovery methods increase the cumulative oil production [33–46]. Among various enhanced oil recovery methods, chemical recovery methods have been widely reported in the literature to enhance porous media's oil production rate [47–51]. Polymer flooding is an efficient method by increasing the water viscosity and helping to more easily mobilize the oil phase through porous media [51–56]. Polyacrylamide (PAM) and partially hydrolyzed polyacrylamide (HPAM) are two of the most functional polymers for enhanced oil recovery processes that help to mobilize the oil phase by increasing water viscosity, wettability alteration, and interfacial tension reduction [57–59]. The following features would be essential in providing efficient

performance during the polymer flooding processes among polymer properties. First, in the polymer solution's carbon chain, there should be no –O– to have more thermal stability. Second, to decrease the rock surface adsorption, a group of negative ionic hydrophilic should be presented in the polymer solution. Third, it should have viscosifying property to provide better performance during polymer flooding processes. Finally, a nonionic hydrophilic group's presence would be a crucial factor in increasing the chemical stability. According to these features, HPAM has provided better results than other polymers during enhanced oil recovery processes [60]. The utilization of nanoparticles regarding their inorganic feature with the organic polymers would be of interest, as it can generate synergy between two materials and improve the oil recovery performances. The creation of hydrogen bonds between the polymers and nanoparticles to enhance the rheological properties of polymer–nanoparticle aqueous solution in the presence of high salinity and temperature is the reason for this phenomenon [61]. The addition of nanoparticles to chemical agents during enhanced oil recovery would be of importance, as it can significantly influence the wettability alteration and reduce the interfacial tension that is combined with the viscosifying property of polymer, which helps the oil phase to be more mobilized through porous media [62–66]. Therefore, the combination of polymer and nanoparticles would be a suitable replacement for conventional chemical enhanced oil recovery methods, such polymer–surfactant and alkaline–polymer–surfactant. Furthermore, the economic costs of nanoparticle preparation would be lower than chemical agents, such as surfactants and foams [67,68]. Ju et al. (2006) and Ogolo et al. (2012) experimentally evaluated the considerable influence of nanoparticle addition on improving oil recovery [69,70]. They concluded that nanoparticles would reduce the interfacial tension, pickering emulsion formation, wettability alteration, and improve the formation stability. This issue has been observed in laboratory conditions to reduce interfacial tension by adding nanoparticles. Table 1 explains a summary of previous literature.

Table 1. A summary of previous hybrid injectivity literature.

Authors	Method	Objectives and Results
Hu et al. (2020) [58]	Saline brines-Foams in sandstone reservoirs	Foam injection after KCl brine has provided a higher recovery factor than another saline brines. It is due to the minimization of monovalent ions in brine.
Piñerez Torrijos et al. (2018) [71]	Hybrid injection of smart water and polymer	Tertiary Low salinity polymer injection has provided higher oil recovery rather than other injectivity scenarios.
Omidi et al. (2020) [72]	Hybrid nanoparticles and surfactant injection	Hybrid injection of nanoparticles and surfactant can provide the highest recovery factor.
Shabib-Asl et al. (2019) [73]	Hybrid injection of low salinity water and foam	Hybrid injection of low salinity water and foam can provide the highest recovery factor.
Rezvani et al. (2020) [74]	Foam stability by nanoparticles with the aim of oil recovery improvement	The foam stability has been improved by the addition of nanoparticles of SiO_2 and Al_2O_3. Therefore, oil recovery has been increased as the foam has been stabilized.

In the present study, we aimed to experimentally evaluate the combined effect of polymer and nanoparticles on oil recovery enhancement. To do this, rheological properties (viscosity), interfacial tension, contact angle, and residual resistance factor in the presence of various nanoparticle concentrations were evaluated in a two-phase flow condition. Furthermore, the effect of polymer and nanoparticles on oil recovery had been sequentially investigated in different scenarios.

2. Materials and Methods

2.1. Materials

2.1.1. Fluids

Crude oil with the viscosity and API gravity of 0.02 and 23° is used in this study. To match the results with the filed applications, synthetic brine with the 6000 mg L^{-1} solution of KCl was prepared. Because KCl can provide equivalent salts, monovalent ions on the polymer stability have been minimized. HPAM (provided by Sigma–Aldrich Co., Steinheim, Germany) was generated with the structure of carboxyl and amide groups with a molecular weight of 7 MDa. The hydrolysis percentage of HPAM is about 30% that was used as a polymer in this study. Al_2O_3 and SiO_2 with a particle size of 7 nm were used comprehensively in previous literature [62–64].

2.1.2. Sandpacks

Sandpacks with an average porosity of 25% and a permeability range of 450–680 mD were prepared. The mineralogical features of Sandpacks have 2% chlorite, 3% kaolinite, 1% illite, and 6% clay. Various grain sizes ranged from 20–140 were sieved to build the artificial sandpacks with reliable petrophysical characteristics. Therefore, the provided sandpacks were adjusted to the reservoir permeability and porosity. Subsequently, the sands were immersed in hydrochloric acid (HCl) with the weight % of 5% for one day to remove the impurities. The sands were dried and packed under 25 MPa to put in the flooding system in the final step.

2.2. Methods

2.2.1. Experimental Apparatus

Figure 1 shows the experimental apparatus for the coreflooding process. It contains the polymer/nanoparticle container, mixed as an aqueous solution before injection into the system. In order to assure that the reservoir temperature would be adopted to the system (333 K), the injection system was put in a heating oven (DZLG-9123A Drying oven, EJER TECH, Pingyao, China). Confining pressure in the system is about 12 MPa. To start the flooding process, 8 PV of oil and synthetic brine with the injection rate of 0.003 m^3/min. were injected to saturate the Sandpacks. Sequential injectivity procedures were performed with the injection rate of 0.001 m^3/min, in the system in order to compare the oil recovery factor for each scenario. Because sandpacks should be dried and cleaned after each test, we used new sandpacks for each test due to the time-consuming process of this operation. The total number of sandpacks was about 20, as we should repeat some tests to validate the results.

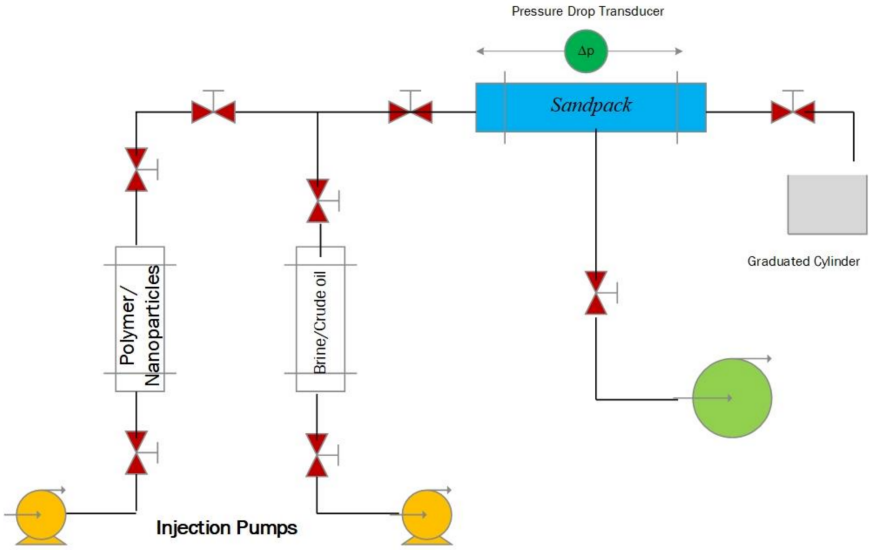

Figure 1. Experimental apparatus for sequential injection of water, polymer, and nanoparticles.

2.2.2. Interfacial Tension

Various nanoparticle concentrations were solved in the polymer as an aqueous phase to measure interfacial tension, and the results were compared with water–SiO_2. To observe the interfacial tension between the aqueous phase and oil, the pendant drop method at the ambient temperature of 298 K was used in laboratory conditions for one day to reach the thermodynamic equilibrium. The equipment was placed in a high-temperature oven (DZLG-9123A Drying oven, EJER TECH, Pingyao, China) to remove the impurities in order to ensure that the procedure has the highest efficiency and the lowest experimental errors.

2.2.3. Residual Resistance Factor

Residual resistance factor is defined as the water opposition to the additional flow (polymer) during polymer injection through porous media, which has caused a decrease in the cross-sectional flow. It can be calculated from the water permeability observation before and after the polymer flooding.

2.2.4. Relative Permeability Curves

Relating the fluid saturation and flow capacity, relative permeability curves are considered to be one of the applicable methods through porous media to indicate the effect of the capillary force. To measure the relative permeabilities for each phase, synthetic brine was injected into the system to obtain the residual oil saturation, and then the polymer–nanoparticle aqueous solution with a pore volume injection of 0.5 was injected. In the final stage, water was injected to produce all the residual oil.

2.2.5. Contact Angle

The samples of outcrop rocks were cleaned with methanol and toluene for two days under the temperature of 333 K to determine the impact of nanoparticles on the capillary forces and wettability alteration. After the samples were cleaned and purified, they were aged by oil to restore as oil-wet that is used for the measurement of contact angle after they submerged in the nanoparticles solutions for one day. The constant stirring is 500 rpm, and the water contact angle was then measured by Layout 2015 software.

2.2.6. Apparent Viscosity Measurement

Polymer solutions were injected at various rates to measure the apparent viscosity. When the steady-state flow had been reached in the system, the apparent polymer viscosity was calculated from the Darcy equation, as follows:

$$v = \frac{Q}{S\phi} \tag{1}$$

where v is the apparent viscosity, S is the core cross-section, Q is the flow rate, and ϕ is the porosity. The shear rate can be calculated from the following equation.

$$\gamma_{pm} = 4\alpha\frac{v}{r} \tag{2}$$

where α has changed according to the reservoir heterogeneity, and it was assumed to be 1.

3. Results and Discussion

3.1. Interfacial Tension

The interfacial tension between oil-water and oil–polymer in the presence of nanoparticle concentration (SiO_2 nanoparticle) was measured in laboratory conditions, as shown in Figure 2. It is evident that, regarding the presence of SiO_2 nanoparticles, interfacial tension has been decreased by increasing nanoparticle concentration for oil–water and oil–polymer. A reduction in the oil–water phase due to the presence of nanoparticles was measured by Sun et al. (2017), which contributed to the Gibbs energy reduction due to the nanoparticles'

placement on the oil–water interface. In contrast, the interfacial tension decreases slightly for oil-polymer as nanoparticle placement on the interface of oil–polymer would be limited, and it caused it to have less interfacial changes by the increase of nanoparticles [75].

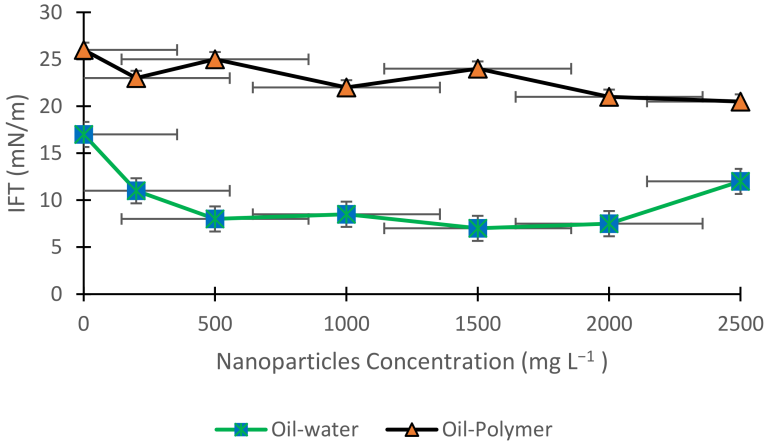

Figure 2. Interfacial tension measurement in the presence of different nanoparticle concentrations.

3.2. Contact Angle

The contact angle is defined as the interface hysteresis, which is affected by the surface roughness. Therefore, the contact angle measurement is performed according to the flat surfaces. The contact angle is an influential parameter for determining wettability alteration, relative permeability curves, and capillary pressure. These parameters have significantly affected the oil recovery performances, as they has been affected by the water–wet or oil–wet property between rock surface and fluid [76,77]. The contact angles were measured for polymer and water treatment on the surface area in the presence of various nanoparticles concentrations (SiO_2 nanoparticle). The contact angle is about 90° when there is no treatment on the rock surface in the initial conditions. It is indicated that the rock surface is water-wet before the treatment processes. After the treatment process with polymer and water, an aqueous phase changes the surface wettability, which caused the increase of nanoparticles to reduce the contact angle. As shown in Figure 3, polymer treatment caused a dramatic decrease rather than a water treatment effect on the contact angle. The minimum contact angles for water and polymer treatment are about 21 and 29, respectively. The contact angle decrease for polymer treatment in the presence of nanoparticles related to the surface hydrophilicity increases. Therefore, after 2000 mg L^{-1} of SiO_2 concentration, there are no significant changes in the contact angle. This concept had been observed and validated from theoretical calculations by previous literature [78–80].

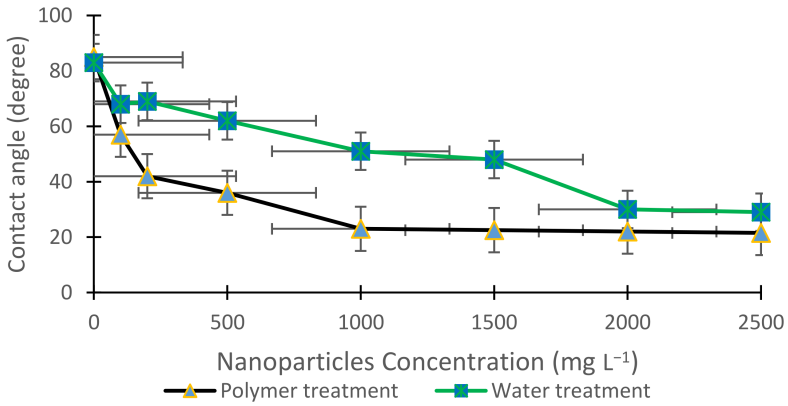

Figure 3. Contact angle measurement in the presence of different nanoparticle concentrations.

3.3. Viscosity

The addition of nanoparticles (SiO_2 and Al_2O_3) in polymer solution would be of an increasing factor on the apparent viscosity. The addition of nanoparticles in polymer solution caused viscosity and shear thinning to increase, as shown in Figure 4. The shear rate is 10 s^{-1} in which can provide reasonable predictions due to the power low model. This phenomenon is related to the flow response of polymer microstructures in previous literature [81–83].

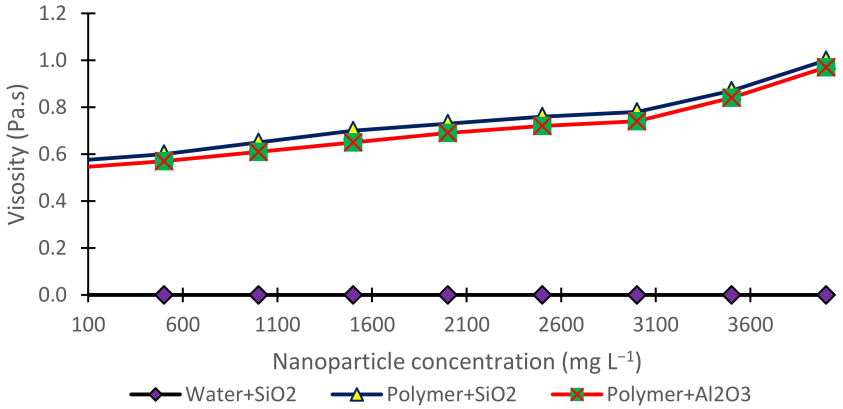

Figure 4. Viscosity measurement in the presence of different nanoparticle concentrations.

3.4. Relative Permeability Curves

Relative permeability curves for water and polymer flooding in the presence of nanoparticles were plotted, as shown in Figure 5. Water relative permeability reduction corresponds to a decrease of residual oil saturation (S_{or}). Therefore, S_{or} and K_{rw} are 29% and 0.3%, respectively, for polymer solution. On the other hand, for a polymer–nanoparticle solution, the S_{or} and K_{rw} are 12% and 0.005%, respectively. Thereby, it is observed that there is an evident reduction for both parameters in the presence and absence of nanoparticles. It has caused capillary forces to decrease and oil recovery increase in the presence of nanoparticles due to the fluid–fluid and rock–fluid interaction. Moreover, S_{or} and K_{rw} alteration at the endpoint corresponds to the wettability alteration from intermediate wet to strongly water wet. This issue was investigated in previous literature to confirm these results [68,84,85].

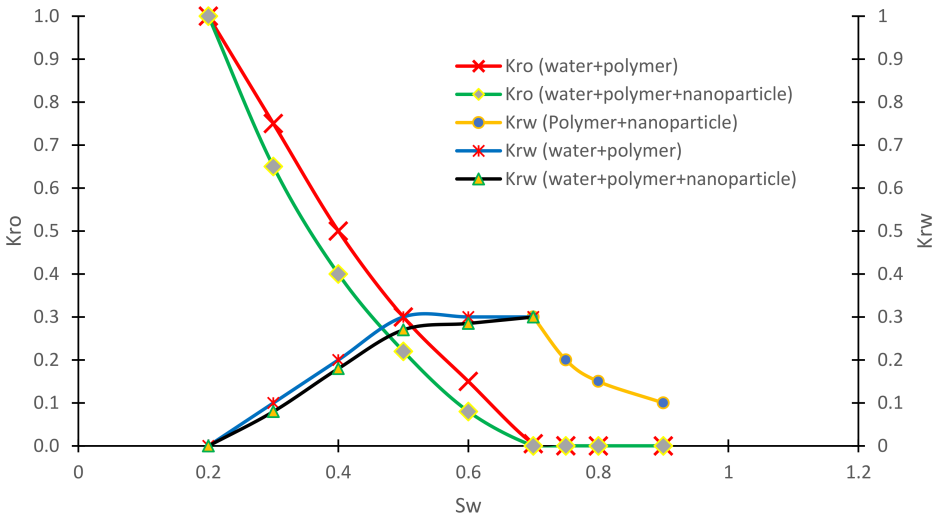

Figure 5. Relative permeability curves for water and polymer flooding in the presence of nanoparticles at reservoir temperature of 60 °C and pressure of 1200 psi.

3.5. Residual Resistance Factor

Residual resistance factor is defined as the comparison factor for determining rock surface contact after and before polymer flooding. It is observed as the rock–fluid interaction and cross-sectional flow reduction. The residual resistance factor has reached a plateau after the shear rate of 100 s^{-1}. It was about three with a reverse pattern with polymer-nanoparticle that is not constant by increasing the shear rate. The polymer solution (HPAM) with a concentration of 500 mg/L was used in this study. For the SiO_2-polymer solution (500 mg/L HPAM and 3000 mg/L of SiO_2), the maximum and minimum residual resistance factors are about 6 and 3.8 Al_2O_3–polymer solution (500 mg/L HPAM and 3000 mg/L of Al_2O_3), it is about 5.5 and 3.2, respectively. The reason for this reduction corresponds to the weak interaction in the anionic sandstone rocks and electrostatic repulsion that resulted in the low polymer retention through porous media [86,87]. It is plotted in Figure 6.

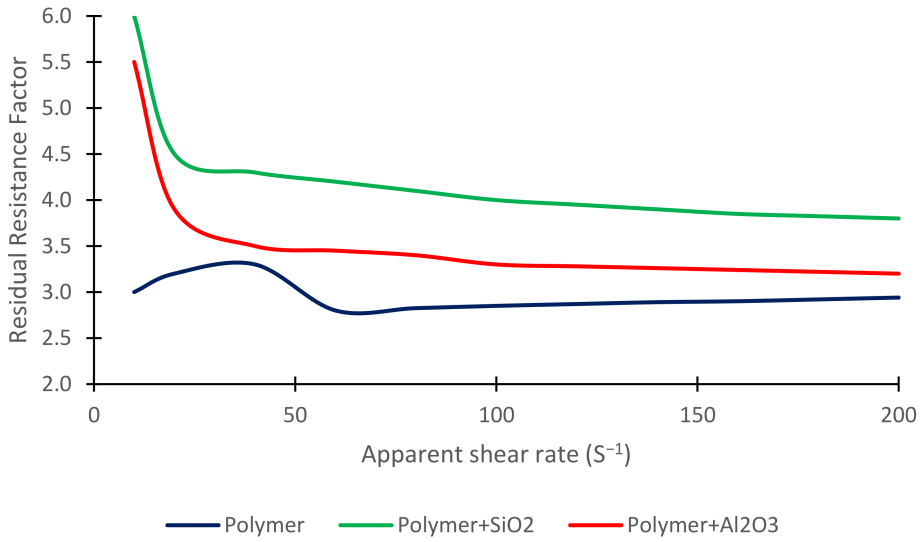

Figure 6. Residual resistance factor versus apparent shear rate for different aqueous solutions at reservoir temperature of 60 °C and pressure of 1200 psi.

3.6. Pressure Drop

Figure 7 shows the pressure drop for water and polymer flooding in the absence of nanoparticles. As is evident, pressure drop has not changed significantly through the pore volume injection, and the maximum pressure drop would be about 0.005 MPa. The pressure drop has fluctuated slightly in the first injection periods for polymer flooding, and it has increased by the increase of pore volume injection. It has its highest value of 0.055 Mpa.

3.7. Oil Recovery Factor

Original oil in place (OOIP) is defined as the total volume of oil in the hydrocarbon reservoir, which is calculated, as follows.

$$OOIP = 7758Vb\ (NTG)\varphi\ S_o/B_o \quad (3)$$

where φ is the porosity, S_o is the oil saturation, Bo is the oil formation volume factor, NTG is the relation of the net to gross volume, and V_b is the bulk volume that can be calculated from the reservoir length and width geometrically. Thereby, the recovery factor is defined as the produced oil versus OOIP, which indicates that porosity directly relates to the porosity [33,88,89]. For higher porosities, oil recovery has been increased as the oil phase can be mobilized more quickly through the porous media. To measure the oil recovery factor, the sequential injection of water and polymer with nanoparticles was performed to measure the oil recovery factor by increasing pore volume injection. Oil recovery for water

flooding, polymer flooding, polymer-Al_2O_3, and polymer-SiO_2 is 48%, 58%, 63%, and 67%, respectively, as shown in Figure 8. Therefore, it is revealed that polymer-SiO_2 flooding would provide better oil recovery than other scenarios, which corresponds to reducing the capillary force due to the structural disjoining pressure.

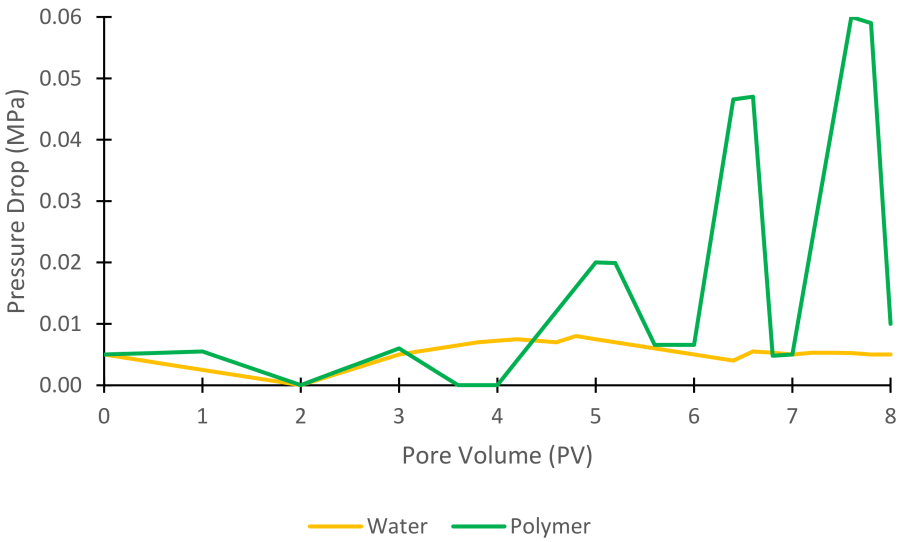

Figure 7. Pressure drop for water and polymer flooding in the absence of nanoparticles.

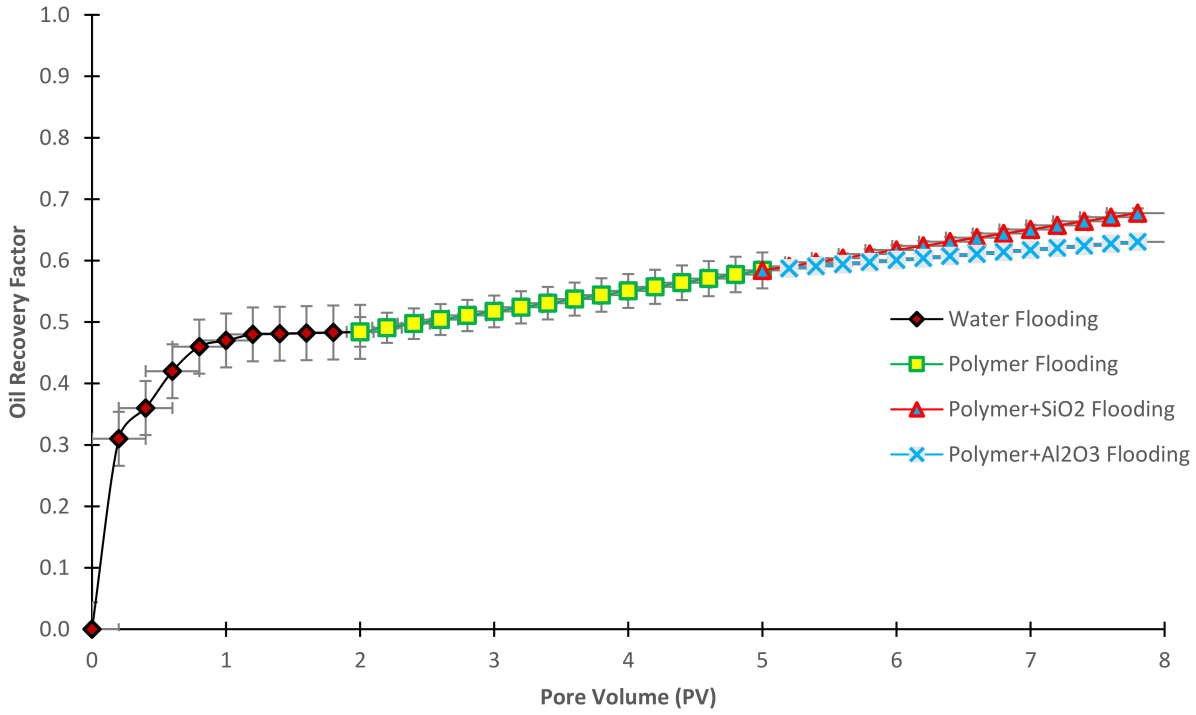

Figure 8. Oil recovery factor for different injectivity scenarios.

3.8. Summary

Table 2 depicts a summary of coreflooding and rheology results.

Table 2. Summary of rheology and coreflooding tests.

	Water Flooding	Polymer Flooding	Polymer Flooding + Al_2O_3	Polymer Flooding + SiO_2
Oil recovery factor (%)	49%	58%	63%	68%
Max K_{ro}	1	/	/	/
Max K_{rw}	/	0.30	/	0.30
Min K_{rw}	/	0.30	/	0.10
S_{ro}	/	0.29	/	0.12
Min RRF	/	2.94	3.20	3.80

4. Conclusions

The enormous demand of various industries for crude oil and its products is vitally essential in enhancing the cumulative oil production from hydrocarbon reservoirs. Oil recovery for water flooding, polymer flooding, polymer–Al_2O_3, and polymer–SiO_2 is 48%, 58%, 63%, and 67%, respectively. Therefore, polymer–SiO_2 flooding would provide better oil recovery than other scenarios, which reduces the capillary force due to the structural disjoining pressure. Moreover, the pressure drop has not changed significantly through the pore volume injection, and the maximum pressure drop would be about 0.005 MPa. The pressure drop has fluctuated slightly in the first injection periods for polymer flooding, and it has increased by the increase of pore volume injection. It has its highest value of 0.055 MPa. The addition of nanoparticles in polymer solution caused the viscosity and shear thinning to increase. This phenomenon is related to the flow response of polymer microstructures.

Regarding the presence of SiO_2 nanoparticles, interfacial tension has been decreased by increasing the nanoparticle concentration for oil–water and oil–polymer. The interfacial tension decreases slightly for oil–polymer, as nanoparticle placement on the interface of oil–polymer would be limited, and it caused to have less interfacial changes by the increase of nanoparticles. Contact angle decrease for polymer treatment in the presence of nanoparticles related to the surface hydrophilicity increase. Therefore, there are no significant changes in contact angle after 2000 mg L^{-1} of SiO_2 concentration.

Author Contributions: Y.H.: Writing—original draft, Methodology, Software; Z.Z.: Formal analysis Investigation; H.D.: Writing—review & editing; M.V.M.: Resources and conceptualization; A.D.: Writing—review & editing, Visualization, Supervision. All authors have read and agreed to the published version of the manuscript.

Funding: This research received no external funding.

Data Availability Statement: There is no data available for this paper.

Acknowledgments: This work was supported by the young talent innovation project of education department of Heilongjiang province of China (Grants No. UNPYSCT-2018114).

Conflicts of Interest: The authors declare no conflict of interest.

References

1. Wang, M.R.; Deng, L.; Liu, G.C.; Wen, L.; Wang, J.G.; Huang, K.B.; Tang, H.T.; Pan, Y.M. Porous organic polymer-derived nanopalladium catalysts for chemoselective synthesis of antitumor benzofuro[2,3-b]pyrazine from 2-Bromophenol and Isonitriles. *Org. Lett.* **2019**. [CrossRef] [PubMed]
2. Zuo, C.; Chen, Q.; Tian, L.; Waller, L.; Asundi, A. Transport of intensity phase retrieval and computational imaging for partially coherent fields: The phase space perspective. *Opt. Lasers Eng.* **2015**. [CrossRef]
3. Zhang, H.; Guan, W.; Zhang, L.; Guan, X.; Wang, S. Degradation of an Organic Dye by Bisulfite Catalytically Activated with Iron Manganese Oxides: The Role of Superoxide Radicals. *ACS Omega* **2020**. [CrossRef] [PubMed]
4. Zhang, H.; Sun, M.; Song, L.; Guo, J.; Zhang, L. Fate of NaClO and membrane foulants during in-situ cleaning of membrane bioreactors: Combined effect on thermodynamic properties of sludge. *Biochem. Eng. J.* **2019**. [CrossRef]

5. Sun, M.; Yan, L.; Zhang, L.; Song, L.; Guo, J.; Zhang, H. New insights into the rapid formation of initial membrane fouling after in-situ cleaning in a membrane bioreactor. *Process Biochem.* **2019**. [CrossRef]
6. Zhang, K.; Huo, Q.; Zhou, Y.Y.; Wang, H.H.; Li, G.P.; Wang, Y.W.; Wang, Y.Y. Textiles/Metal-Organic Frameworks Composites as Flexible Air Filters for Efficient Particulate Matter Removal. *ACS Appl. Mater. Interfaces* **2019**. [CrossRef]
7. Duan, Z.; Li, C.; Zhang, Y.; Dong, L.; Bai, X.; Yang, M.; Jia, D.; Li, R.; Cao, H.; Xu, X. Milling surface roughness for 7050 aluminum alloy cavity influenced by nozzle position of nanofluid minimum quantity lubrication. *Chin. J. Aeronaut.* **2020**. [CrossRef]
8. Zhang, J.; Wu, W.; Li, C.; Yang, M.; Zhang, Y.; Jia, D.; Hou, Y.; Li, R.; Cao, H.; Ali, H.M. Convective Heat Transfer Coefficient Model Under Nanofluid Minimum Quantity Lubrication Coupled with Cryogenic Air Grinding Ti–6Al–4V. *Int. J. Precis. Eng. Manuf. Green Technol.* **2020**. [CrossRef]
9. Gao, T.; Li, C.; Jia, D.; Zhang, Y.; Yang, M.; Wang, X.; Cao, H.; Li, R.; Ali, H.M.; Xu, X. Surface morphology assessment of CFRP transverse grinding using CNT nanofluid minimum quantity lubrication. *J. Clean. Prod.* **2020**. [CrossRef]
10. Sui, M.; Li, C.; Wu, W.; Yang, M.; Ali, H.M.; Zhang, Y.; Jia, D.; Hou, Y.; Li, R.; Cao, H. Temperature of Grinding Carbide with Castor Oil-Based MoS2 Nanofluid Minimum Quantity Lubrication. *J. Therm. Sci. Eng. Appl.* **2021**. [CrossRef]
11. Mao, Q.F.; Shang-Guan, Z.F.; Chen, H.L.; Huang, K. Immunoregulatory role of IL-2/STAT5/CD4+ CD25+ Foxp3 Treg pathway in the pathogenesis of chronic osteomyelitis. *Ann. Transl. Med.* **2019**, *7*. [CrossRef]
12. Huang, K.; Ge, S. The anti-CXCL4 antibody depletes CD4 (+) CD25 (+) FOXP3 (+) regulatory T cells in CD4+ T cells from chronic osteomyelitis patients by the STAT5 pathway. *Ann. Palliat. Med.* **2020**, *9*, 2723–2730. [CrossRef]
13. Zheng, Y.; Yu, Y.; Lin, W.; Jin, Y.; Yong, Q.; Huang, C. Enhancing the enzymatic digestibility of bamboo residues by biphasic phenoxyethanol-acid pretreatment. *Bioresour. Technol.* **2021**, *325*, 124691. [CrossRef]
14. Peng, X.; He, H.; Liu, Q.; She, K.; Zhang, B.; Wang, H.; Pan, Y. Photocatalyst-Controlled and Visible Light-Enabled Selective Oxidation of Pyridinium Salts. *Sci. China Chem.* **2021**. [CrossRef]
15. Huang, C.; Zheng, Y.; Lin, W.; Shi, Y.; Huang, G.; Yong, Q. Removal of fermentation inhibitors from pre-hydrolysis liquor using polystyrene divinylbenzene resin. *Biotechnol. Biofuels* **2020**, *13*, 1–14. [CrossRef]
16. Lin, W.; Xing, S.; Jin, Y.; Lu, X.; Huang, C.; Yong, Q. Insight into understanding the performance of deep eutectic solvent pretreatment on improving enzymatic digestibility of bamboo residues. *Bioresour. Technol.* **2020**, *306*, 123163. [CrossRef]
17. Zhang, Y.; Li, C.; Jia, D.; Zhang, D.; Zhang, X. Experimental evaluation of the lubrication performance of MoS2/CNT nanofluid for minimal quantity lubrication in Ni-based alloy grinding. *Int. J. Mach. Tools Manuf.* **2015**. [CrossRef]
18. Zuo, C.; Sun, J.; Li, J.; Zhang, J.; Asundi, A.; Chen, Q. High-resolution transport-of-intensity quantitative phase microscopy with annular illumination. *Sci. Rep.* **2017**. [CrossRef]
19. Huang, W.Y.; Wang, G.Q.; Li, W.H.; Li, T.T.; Ji, G.-j.; Ren, S.-C.; Jiang, M.; Yan, L.; Tang, H.-T.; Pan, Y.-M.; et al. Porous Ligand Creates New Reaction Route: Bifunctional Single-Atom Palladium Catalyst for Selective Distannylation of Terminal Alkynes. *Chem* **2020**. [CrossRef]
20. Qiao, Y.-X.; Sheng, S.-L.; Zhang, L.-M.; Chen, J.; Yang, L.-L.; Zhou, H.-L.; Wang, Y.-X.; Li, H.-B.; Zheng, Z.-B. Friction and wear behaviors of a high nitrogen austenitic stainless steel Fe-19Cr-15Mn-0.66N. *J. Min. Metall. Sect. B Metall.* **2021**. [CrossRef]
21. Wang, P.; Li, Z.; Xie, Q.; Duan, W.; Zhang, X.; Han, H. A Passive Anti-icing Strategy Based on a Superhydrophobic Mesh with Extremely Low Ice Adhesion Strength. *J. Bionic. Eng.* **2021**. [CrossRef]
22. Kazemi, A.; Yang, S. Effects of magnesium dopants on grain boundary migration in aluminum-magnesium alloys. *Comput. Mater. Sci.* **2021**. [CrossRef]
23. Kazemi, A.; Yang, S. Atomistic Study of the Effect of Magnesium Dopants on the Strength of Nanocrystalline Aluminum. *JOM* **2019**. [CrossRef]
24. Zheng, L.; Yu, P.; Zhang, Y.; Wang, P.; Yan, W.; Guo, B.; Huang, C.; Jiang, Q. Evaluating the bio-application of biomacromolecule of lignin-carbohydrate complexes (LCC) from wheat straw in bone metabolism via ROS scavenging. *Int. J. Biol. Macromol.* **2021**. [CrossRef]
25. Davarpanah, A.; Mirshekari, B.; Jafari Behbahani, T.; Hemmati, M. Integrated production logging tools approach for convenient experimental individual layer permeability measurements in a multi-layered fractured reservoir. *J. Pet. Explor. Prod. Technol.* **2018**. [CrossRef]
26. Hu, X.; Li, M.; Peng, C.; Davarpanah, A. Hybrid Thermal-Chemical Enhanced Oil Recovery Methods; An Experimental Study for Tight Reservoirs. *Symmetry* **2020**, *12*, 947. [CrossRef]
27. Davarpanah, A. Parametric study of polymer-nanoparticles-assisted injectivity performance for axisymmetric two-phase flow in EOR processes. *Nanomaterials* **2020**, *10*, 1818. [CrossRef]
28. Hu, X.; Xie, J.; Cai, W.; Wang, R.; Davarpanah, A. Thermodynamic effects of cycling carbon dioxide injectivity in shale reservoirs. *J. Pet. Sci. Eng.* **2020**. [CrossRef]
29. Davarpanah, A. A feasible visual investigation for associative foam >\ polymer injectivity performances in the oil recovery enhancement. *Eur. Polym. J.* **2018**. [CrossRef]
30. Yang, Y.; Yao, J.; Wang, C.; Gao, Y.; Zhang, Q.; An, S.; Song, W. New pore space characterization method of shale matrix formation by considering organic and inorganic pores. *J. Nat. Gas. Sci. Eng.* **2015**. [CrossRef]
31. Zhang, K.; Zhang, J.; Ma, X.; Yao, C.; Zhang, L.; Yang, Y.; Wang, J.; Yao, J.; Zhao, H. History Matching of Naturally Fractured Reservoirs Using a Deep Sparse Autoencoder. *SPE J.* **2021**. [CrossRef]

32. Nesic, S.; Zolotukhin, A.; Mitrovic, V.; Govedarica, D.; Davarpanah, A. An Analytical Model to Predict the Effects of Suspended Solids in Injected Water on the Oil Displacement Efficiency during Waterflooding. *Processes* **2020**, *8*, 659. [CrossRef]
33. Davarpanah, A.; Mirshekari, B. Experimental Investigation and Mathematical Modeling of Gas Diffusivity by Carbon Dioxide and Methane Kinetic Adsorption. *Ind. Eng. Chem. Res.* **2019**. [CrossRef]
34. Mazarei, M.; Davarpanah, A.; Ebadati, A.; Mirshekari, B. The feasibility analysis of underground gas storage during an integration of improved condensate recovery processes. *J. Pet. Explor. Prod. Technol.* **2019**. [CrossRef]
35. Pan, F.; Zhang, Z.; Zhang, X.; Davarpanah, A. Impact of anionic and cationic surfactants interfacial tension on the oil recovery enhancement. *Powder Technol.* **2020**. [CrossRef]
36. Jia, K.; Feng, Q.; Davarpanah, A. Effect of anionic and non-anionic surfactants on the adsorption density. *Pet. Sci. Technol.* **2021**. [CrossRef]
37. Esfandyari, H.; Moghani, A.; Esmaeilzadeh, F.; Davarpanah, A. A Laboratory Approach to Measure Carbonate Rocks' Adsorption Density by Surfactant and Polymer. *Math. Probl. Eng.* **2021**. [CrossRef]
38. Sepahvand, T.; Etemad, V.; Matinizade, M.; Shirvany, A. Symbiosis of AMF with growth modulation and antioxidant capacity of Caucasian Hackberry (Celtis Caucasica L.) seedlings under drought stress. *Cent. Asian J. Environ. Sci. Technol. Innov.* **2021**, *2*. [CrossRef]
39. Jalali Sarvestani, M.; Charehjou, P. Fullerene (C20) as a potential adsorbent and sensor for the removal and detection of picric acid contaminant: DFT Studies. *Cent. Asian J. Environ. Sci. Technol. Innov.* **2021**, *2*. [CrossRef]
40. Awan, B.; Sabeen, M.; Shaheen, S.; Mahmood, Q.; Ebadi, A.; Toughani, M. Phytoextraction of zinc contaminated water by *Tagetes minuta* L. *Cent. Asian J. Environ. Sci. Technol. Innov.* **2020**, *1*, 150–158. [CrossRef]
41. Bafkar, A. Kinetic and equilibrium studies of adsorptive removal of sodium-ion onto wheat straw and rice husk wastes. *Cent. Asian J. Environ. Sci. Technol. Innov.* **2020**, *1*. [CrossRef]
42. Maina, Y.; Kyari, B.; Jimme, M. Impact of household fuel expenditure on the environment: The quest for sustainable energy in Nigeria. *Cent. Asian J. Environ. Sci. Technol. Innov.* **2020**, *1*, 109–118. [CrossRef]
43. Nwankwo, C.; EGobo, A.; Israel-Cookey, C.; AAbere, S. Effects of hazardous waste discharge from the activities of oil and gas companies in Nigeria. *Cent. Asian J. Environ. Sci. Technol. Innov.* **2020**, *1*, 119–129. [CrossRef]
44. Qayyum, S.; Khan, I.; Meng, K.; Zhao, Y.; Peng, C. A review on remediation technologies for heavy metals contaminated soil. *Cent. Asian J. Environ. Sci. Technol. Innov.* **2020**, *1*, 21–29. [CrossRef]
45. Ebadi, A.; Toughani, M.; Najafi, A.; Babaee, M. A brief overview on current environmental issues in Iran. *Cent. Asian J. Environ. Sci. Technol. Innov.* **2020**, *1*, 1–11. [CrossRef]
46. Nnaemeka, A. Environmental pollution and associated health hazards to host communities (Case study: Niger delta region of Nigeria). *Cent. Asian J. Environ. Sci. Technol. Innov.* **2020**, *1*, 30–42. [CrossRef]
47. Firozjaii, A.M.; Saghafi, H.R. Review on chemical enhanced oil recovery using polymer flooding: Fundamentals, experimental and numerical simulation. *Petroleum* **2020**. [CrossRef]
48. Mandal, A. Chemical flood enhanced oil recovery: A review. *Int. J. Oil Gas Coal Technol.* **2015**. [CrossRef]
49. Gurgel, A.; Moura, M.C.P.A.; Dantas, T.N.C.; Neto, E.B.; Neto, A.D. A Review on Chemical Flooding Methods Applied in Enhanced Oil Recovery. *Braz. J. Pet. Gas* **2008**. [CrossRef]
50. Davarpanah, A.; Mirshekari, B. Mathematical modeling of injectivity damage with oil droplets in the waste produced water re-injection of the linear flow. *Eur. Phys. J. Plus* **2019**. [CrossRef]
51. Davarpanah, A.; Shirmohammadi, R.; Mirshekari, B.; Aslani, A. Analysis of hydraulic fracturing techniques: Hybrid fuzzy approaches. *Arabian J. Geosci.* **2019**. [CrossRef]
52. Esfandyari, H.; Moghani Rahimi, A.; Esmaeilzadeh, F.; Davarpanah, A.; Mohammadi, A.H. Amphoteric and cationic surfactants for enhancing oil recovery from carbonate oil reservoirs. *J. Mol. Liq.* **2020**. [CrossRef]
53. Davarpanah, A.; Mirshekari, B. Numerical simulation and laboratory evaluation of alkali–surfactant–polymer and foam flooding. *Int. J. Environ. Sci. Technol.* **2019**. [CrossRef]
54. Davarpanah, A.; Mirshekari, B. Experimental study of CO_2 solubility on the oil recovery enhancement of heavy oil reservoirs. *J. Therm. Anal. Calorim.* **2019**. [CrossRef]
55. Esfandyari, H.; Shadizadeh, S.R.; Esmaeilzadeh, F.; Davarpanah, A. Implications of anionic and natural surfactants to measure wettability alteration in EOR processes. *Fuel* **2020**. [CrossRef]
56. Davarpanah, A.; Mirshekari, B. A mathematical model to evaluate the polymer flooding performances. *Energy Rep.* **2019**. [CrossRef]
57. Esfandyari, H.; Hoseini, A.H.; Shadizadeh, S.R.; Davarpanah, A. Simultaneous evaluation of capillary pressure and wettability alteration based on the USBM and imbibition tests on carbonate minerals. *J. Pet. Sci. Eng.* **2020**. [CrossRef]
58. Hu, Y.; Cheng, Q.; Yang, J.; Zhang, L.; Davarpanah, A. A laboratory approach on the hybrid-enhanced oil recovery techniques with different saline brines in sandstone reservoirs. *Processes* **2020**, *8*, 1051. [CrossRef]
59. Davarpanah, A.; Shirmohammadi, R.; Mirshekari, B. Experimental evaluation of polymer-enhanced foam transportation on the foam stabilization in the porous media. *Int. J. Environ. Sci. Technol.* **2019**. [CrossRef]

60. Davarpanah, A.; Akbari, E.; Doudman-Kushki, M.; Ketabi, H.; Hemmati, M. Simultaneous feasible injectivity of foam and hydrolyzed polyacrylamide to optimize the oil recovery enhancement. *Energy Explor. Exploit.* **2019**. [CrossRef]
61. Haiyan, Z.; Davarpanah, A. Hybrid Chemical Enhanced Oil Recovery Techniques: A Simulation Study. *Symmetry* **2020**, *12*, 1086. [CrossRef]
62. Sheng, J.J. Modern Chemical Enhanced Oil Recovery. *Mod. Chem. Enhanc. Oil Recover.* **2011**. [CrossRef]
63. Hu, Z.; Haruna, M.; Gao, H.; Nourafkan, E.; Wen, D. Rheological Properties of Partially Hydrolyzed Polyacrylamide Seeded by Nanoparticles. *Ind. Eng. Chem. Res.* **2017**. [CrossRef]
64. Agista, M.N.; Guo, K.; Yu, Z. A state-of-the-art review of nanoparticles application in petroleum with a focus on enhanced oil recovery. *Appl. Sci.* **2018**, *8*, 871. [CrossRef]
65. Shamsijazeyi, H.; Miller, C.A.; Wong, M.S.; Tour, J.M.; Verduzco, R. Polymer-coated nanoparticles for enhanced oil recovery. *J. Appl. Polym. Sci.* **2014**. [CrossRef]
66. Ali, J.A.; Kolo, K.; Manshad, A.K.; Mohammadi, A.H. Recent advances in application of nanotechnology in chemical enhanced oil recovery: Effects of nanoparticles on wettability alteration, interfacial tension reduction, and flooding. *Egypt J. Pet.* **2018**. [CrossRef]
67. Cheraghian, G.; Hendraningrat, L. A review on applications of nanotechnology in the enhanced oil recovery part B: Effects of nanoparticles on flooding. *Int. Nano Lett.* **2016**. [CrossRef]
68. Ali, J.A.; Kalhury, A.M.; Sabir, A.N.; Ahmed, R.N.; Ali, N.H.; Abdullah, A.D. A state-of-the-art review of the application of nanotechnology in the oil and gas industry with a focus on drilling engineering. *J. Pet. Sci. Eng.* **2020**. [CrossRef]
69. Ju, B.; Fan, T.; Ma, M. Enhanced oil recovery by flooding with hydrophilic nanoparticles. *China Particuology* **2006**. [CrossRef]
70. Ogolo, N.A.; Olafuyi, O.A.; Onyekonwu, M.O. Enhanced oil recovery using nanoparticles. *Soc. Pet. Eng. SPE Saudi Arab. Sect. Tech. Symp. Exhib.* **2012**. [CrossRef]
71. Piñerez Torrijos, I.D.; Puntervold, T.; Strand, S.; Austad, T.; Bleivik, T.H.; Abdullah, H.I. An experimental study of the low salinity Smart Water—Polymer hybrid EOR effect in sandstone material. *J. Pet. Sci. Eng.* **2018**. [CrossRef]
72. Omidi, A.; Manshad, A.K.; Moradi, S.; Ali, J.A.; Sajadi, S.M.; Keshavarz, A. Smart- and nano-hybrid chemical EOR flooding using Fe_3O_4/eggshell nanocomposites. *J. Mol. Liq.* **2020**. [CrossRef]
73. Shabib-Asl, A.; Abdalla Ayoub, M.; Abdalla Elraies, K. Combined low salinity water injection and foam flooding in sandstone reservoir rock: A new hybrid EOR. In Proceedings of the SPE Middle East Oil and Gas Show and Conference, Manama, Bahrain, 18–21 March 2019. [CrossRef]
74. Rezvani, H.; Panahpoori, D.; Riazi, M.; Parsaei, R.; Tabaei, M.; Cortés, F.B. A novel foam formulation by Al_2O_3/SiO_2 nanoparticles for EOR applications: A mechanistic study. *J. Mol. Liq.* **2020**. [CrossRef]
75. Maghzi, A.; Mohebbi, A.; Kharrat, R.; Ghazanfari, M.H. An experimental investigation of silica nanoparticles effect on the rheological behavior of polyacrylamide solution to enhance heavy oil recovery. *Pet. Sci. Technol.* **2013**. [CrossRef]
76. Gbadamosi, A.O.; Junin, R.; Manan, M.A.; Agi, A.; Oseh, J.O.; Usman, J. Effect of aluminium oxide nanoparticles on oilfield polyacrylamide: Rheology, interfacial tension, wettability and oil displacement studies. *J. Mol. Liq.* **2019**. [CrossRef]
77. Ahmed, A.; Saaid, I.M.; Ahmed, A.A.; Pilus, R.M.; Baig, M.K. Evaluating the potential of surface-modified silica nanoparticles using internal olefin sulfonate for enhanced oil recovery. *Pet. Sci.* **2020**. [CrossRef]
78. Sun, X.; Zhang, Y.; Chen, G.; Gai, Z. Application of nanoparticles in enhanced oil recovery: A critical review of recent progress. *Energies* **2017**, *10*, 345. [CrossRef]
79. Gbadamosi, A.O.; Junin, R.; Manan, M.A.; Yekeen, N.; Agi, A.; Oseh, J.O. Recent advances and prospects in polymeric nanofluids application for enhanced oil recovery. *J. Ind. Eng. Chem.* **2018**. [CrossRef]
80. Ali, H.; Soleimani, H.; Yahya, N.; Khodapanah, L.; Sabet, M.; Demiral, B.M.R.; Hussain, T.; Adebayo, L.L. Enhanced oil recovery by using electromagnetic-assisted nanofluids: A review. *J. Mol. Liq.* **2020**. [CrossRef]
81. Gbadamosi, A.O.; Junin, R.; Manan, M.A.; Agi, A.; Oseh, J.O.; Usman, J. Synergistic application of aluminium oxide nanoparticles and oilfield polyacrylamide for enhanced oil recovery. *J. Pet. Sci. Eng.* **2019**. [CrossRef]
82. Maurya, N.K.; Mandal, A. Studies on behavior of suspension of silica nanoparticle in aqueous polyacrylamide solution for application in enhanced oil recovery. *Pet. Sci. Technol.* **2016**. [CrossRef]
83. Cheraghian, G.; Khalili Nezhad, S.S.; Kamari, M.; Hemmati, M.; Masihi, M.; Bazgir, S. Adsorption polymer on reservoir rock and role of the nanoparticles, clay and SiO_2. *Int. Nano Lett.* **2014**. [CrossRef]
84. Saha, R.; Uppaluri, R.V.S.; Tiwari, P. Impact of Natural Surfactant (Reetha), Polymer (Xanthan Gum), and Silica Nanoparticles to Enhance Heavy Crude Oil Recovery. *Energy Fuels* **2019**. [CrossRef]
85. Sharma, T.; Iglauer, S.; Sangwai, J.S. Silica Nanofluids in an Oilfield Polymer Polyacrylamide: Interfacial Properties, Wettability Alteration, and Applications for Chemical Enhanced Oil Recovery. *Ind. Eng. Chem. Res.* **2016**. [CrossRef]
86. Lee, J.; Huang, J.; Babadagli, T. Visual support for heavy-oil emulsification and its stability for cold-production using chemical and nano-particles. In Proceedings of the SPE Annual Technical Conference and Exhibition, Calgary, AB, Canada, 30 September–2 October 2019. [CrossRef]
87. Cheraghian, G. Evaluation of clay and fumed silica nanoparticles on adsorption of surfactant polymer during enhanced oil recovery. *J. Jpn. Pet. Inst.* **2017**. [CrossRef]

88. Samba, M.A.; Hassan, H.A.; Munayr, M.S.; Yusef, M.; Eschweido, A.; Burkan, H.; Elsharafi, M.O. Nanoparticles EOR aluminum oxide (Al_2O_3) used as a spontaneous imbibition test for sandstone core. In Proceedings of the ASME International Mechanical Engineering Congress and Exposition, Salt Lake City, UT, USA, 11–14 November 2019. [CrossRef]
89. Daryayehsalameh, B.; Nabavi, M.; Vaferi, B. Modeling of CO_2 capture ability of [Bmim][BF4] ionic liquid using connectionist smart paradigms. *Environ. Technol. Innov.* **2021**, *22*, 101484. [CrossRef]